sustainability

MDPI

Article

Assessing Hydrological Response and Resilience of Watersheds as Strategy for Climatic Change Adaptation in Neotropical Region

Matheus E. K. Ogasawara [1,*], Eduardo M. Mattos [2], Humberto R. Rocha [3], Xiaohua Wei [4] and Silvio F. B. Ferraz [1]

[1] Forest Hydrology Laboratory, Department of Forest Sciences, Luiz de Queiroz College of Agriculture, University of São Paulo, Piracicaba 13418-900, Brazil; silvio.ferraz@usp.br
[2] Geplant Forest Technology Ltd., Piracicaba 13418-360, Brazil; eduardo@geplant.com.br
[3] Department of Atmospheric Sciences, Institute of Astronomy, Geophysics and Atmospheric Sciences, University of São Paulo, São Paulo 05508-220, Brazil; humberto.rocha@iag.usp.br
[4] Department of Earth & Environmental Sciences, The University of British Columbia, Kelowna, BC V1V 1V7, Canada; adam.wei@ubc.ca
* Correspondence: matheus.ogasawara@usp.br

Abstract: This study aimed to assess the hydrological response and resilience of watersheds in a neotropical region to identify regions sensitive to climate variations, enabling the development of adaptive strategies in response to global environmental changes. This study applied Budyko's framework using Fuh's hydrological model rewritten by Zhou to estimate hydrological response and Budyko's metrics (deviation and elasticity) to estimate hydrological resilience to climatic changes in 26 watersheds in southeastern Brazil. The proposed modeling was able to capture the differences among the watersheds, with "m" values ranging from 1.79 to 3.63. It was possible to rank the hydrological resilience from low to high across watersheds using Budyko's metrics, where the highest values of elasticity were found in watersheds with a higher percentage of forest cover. The sensitive analyses showed that watersheds with higher "m" values are more sensitive to changes in precipitation and potential evapotranspiration. The results also demonstrate that mean elevation and stream density were two key variables that influence the "m" value; these physiographic characteristics may alter the water and energy balance of the watershed affecting the water yield. A relationship between watershed's hydrological response and resilience was proposed to identify critical areas for the stability of water yield in the watersheds, providing a guide for public policy and suggesting ways to help the management of water resources in watersheds.

Keywords: hydrological model; water resource; climate change; watershed resilience

Citation: Ogasawara, M.E.K.; Mattos, E.M.; Rocha, H.R.; Wei, X.; Ferraz, S.F.B. Assessing Hydrological Response and Resilience of Watersheds as Strategy for Climatic Change Adaptation in Neotropical Region. *Sustainability* **2024**, *16*, 8910. https://doi.org/10.3390/su16208910

Academic Editor: Lucio Di Matteo

Received: 30 August 2024
Revised: 2 October 2024
Accepted: 8 October 2024
Published: 15 October 2024

1. Introduction

Global warming has been increased by the anthropic emission of greenhouse gasses, modifying the hydrological cycle, accelerating evapotranspiration, and altering the rainfall regime [1]. The neotropical region has warmed by 0.7 °C over the past fifty years, and this increase may cause damage to ecosystems, food production, and energy generation [2]. Climate change is impacting water availability and watershed resilience given its dependence on climate conditions and seasonality [3–5]. Currently, global problems faced by the population include droughts and floods, related to global changes in climate and land use, which interfere in the availability of water [2].

Global alterations in climate and land use are widely acknowledged as primary drivers of hydrological variability. Consequently, their interplay holds the potential to exert a significant impact on the future dynamics of water supply and flow regimes. Models derived from Budyko's framework, capable of simultaneously integrating the physiographic features of watersheds and climatic variables, are essential for an informed assessment of future water resources [4,6–12]. Within this context, hydrological models

assume a pivotal role in predicting water and energy balances for unmonitored watersheds, a critical concern in contemporary hydrology [13].

Hydrological models are able to simulate future climate scenarios, making it possible to estimate water yield and consequently assist in the creation of public policies for sustainable water use and management [2]. Simulations of future climate scenarios in South America have identified trends of a reduction in flows in the north and northeast regions, while for the south and southeast regions, there is an increase, and these variations are directly related to variations in precipitation [14,15]. Hydrological models based on Budyko's framework [16,17] have been created, adapted, and used to predict water and energy balances in watersheds [18], such as the models of Turc [19] and Pike [20], which are empirical equations that do not take into account the physiographic features of the watershed, such as topography, forest cover, and soil properties. Thus, in order to improve those models, some studies have suggested adding an adjustable parameter, "m" or "n", which represents the characteristics of the watershed, the "second generation of equations based on Budyko's framework" [4,6,7,11], and Fuh's model rewritten by Zhou [4] is the only one that has streamflow as an independent variable.

Another tool used to assess the effects of climate change is the calculation of some of Budyko's metrics such as dynamic deviation and elasticity, which measure the hydrological resilience of the watershed [3], which represents the ability to absorb change and maintain or recover its hydrological function quickly after a disturbance such as drought [3,21]. Hydrologically resilient watersheds are those with stability and/or predictability of water yield in the face of changes in environmental conditions (e.g., climate changes), while non-resilient watersheds are subject to undergo changes in water yield, affecting water availability to the population [3]. In contrast to previous studies that focused exclusively on Budyko's metrics [3,22] or only on hydrological models [4,6,7,11], the combination of both methods may offer a valuable approach for the conservation and management of water resources, especially in the context of climate change. This integrated approach not only enhances the understanding and prediction of fluctuations in water availability but also provides critical insights into water resource dynamics in the watershed.

The southeastern region of Brazil encompasses a range of climate zones, resulting in varied hydrological responses. This region frequently experiences water scarcity issues, exacerbated by land use changes driven by agriculture, urbanization, and deforestation, and climate change, including altered precipitation patterns and an increased frequency of extreme weather events. Integrating Budyko's metrics with hydrological models may provide a comprehensive framework for understanding and managing the complex dynamics of water resources in southeastern Brazil. The effects of climate change on water resources in this region are projected to materialize in the coming years, as documented in several scientific studies [2,5,14]. Therefore, identifying watersheds that exhibit vulnerability to these changes is crucial, particularly within tropical regions that are likely to experience the initial and most pronounced effects of climate change [23].

In this context, the objective of this study was to assess the hydrological response and resilience of watersheds in southeastern Brazil in order to identify regions characterized by sensitivity to climate variations, thereby facilitating the establishment of an adaptive strategy in response to global environmental changes. Therefore, quantifying the potential changes in water resources under climate change and their physiographic features is important for water managers and policy-makers to develop sustainable water resource strategies for this region, especially in tropical and subtropical regions, where the effects of climate change are expected to be among the earliest to emerge.

2. Materials and Methods

2.1. Study Area

This study covers the southeastern region of Brazil, including the states of São Paulo, Minas Gerais, and Paraná. The population of this region is around 80 million, approximately 40% of the total population of Brazil. In addition, the southeastern region encompasses

the main economic activities, and it is also responsible for more than 65% of the country's hydroelectric plants [24], and urban and industrial concentrations in this region are critical factors to guide public policy planning and propose ways to manage and conserve water resources in watersheds. In this context, the watersheds of this study were selected according to the criteria of the availability of climatic and discharge data, considering only time series with at least 10 years of data, not necessarily consecutive, in different streams, avoiding two points in the same river. Köppen–Geiger climatic classification at the regional scale is shown in Figure 1 [25]. The average annual precipitation ranged between 1235 mm and 1612 mm, and the average annual temperature ranged between 21 °C and 25 °C across the watersheds.

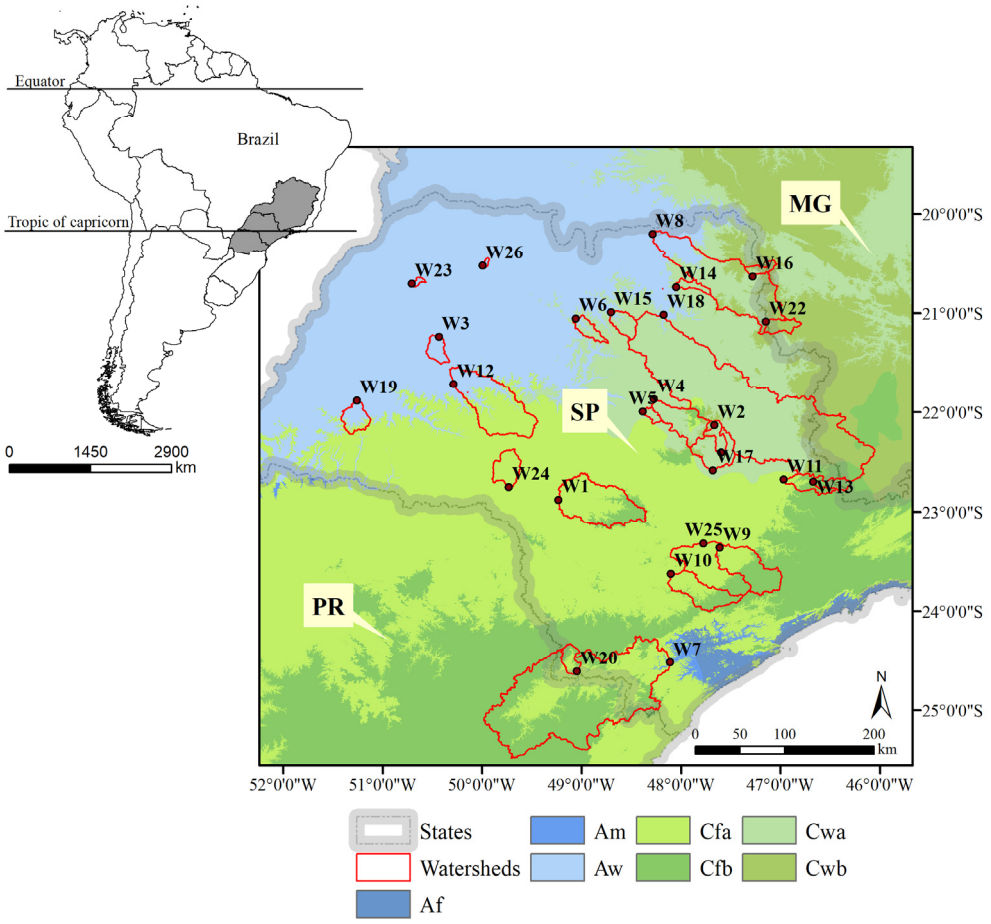

Figure 1. Location of 26 long-term monitoring watersheds selected for this study (W1–W26). Köppen–Geiger climate classification for the studied watersheds. (A) Tropical (f) without dry season, (m) monsoon, (w) with dry winter, (C) humid subtropical, (fa) oceanic climate, without dry season, with hot summer, (fb) oceanic climate, without dry season, with temperate summer, (wa) with dry winter and hot summer, (wb) with dry winter and temperate summer. SP, MG, and PR represent the states of São Paulo, Minas Gerais, and Paraná, respectively.

2.2. Physiographic Features and Land Use of Watersheds

To characterize the 26 watersheds, the hydrographic network of the 26 watersheds was extracted from the multi-scale ottocodified hydrographic base of ANA (Agência Nacional de Águas—National water agency) [26] with a scale of 1:50,000. Stream density was calculated by dividing the linear extension of the hydrographic network by the area of each watershed. Elevation was obtained using the digital elevation model (DEM), with a spatial resolution of 30 m, created from the SRTM (Shuttle Radar Topography Mission) of USGS (United States Geological Survey) [27]. The maximum, average, and minimum elevation values, as well as the maximum, average, and minimum slope (in %) of each

watershed, were obtained from the DEM. Soil texture was obtained from the SoilGrids database with a spatial resolution of 250 m [28]. The average vertical distance to the nearest drain (HAND—height above the nearest drainage) is a measure indirectly related to soil depth and was obtained from the AMBDATA database using a threshold of 50 pixels with a spatial resolution of 30 arc seconds [29] (Table 1).

Table 1. Physiographic features of 26 watersheds: area, stream density, soil texture, elevation, slope, hand, and percentage of different land uses of watersheds for the year 2018; 'NDVI' represents the mean (dry and wet season) normalized difference vegetation index for the native forest. The land use "others" represents non-forest natural formation.

Watershed	Area	Stream Density	Clay	Silt	Sand	Elevation			Slope	HAND	Land Use				NDVI
						Max	Mean	Min	Mean	Mean	Agriculture	Urban	Forest	Others	
	km²	km km^{-2}		%			m		%	cm		%			
W 1	3344	2.5	35	17	48	1004	765	526	3	54	52	1	44	3	0.44
W 2	66	1.7	33	14	53	1052	853	656	7	142	70	1	28	1	0.47
W 3	471	2.2	21	12	67	514	433	351	3	41	96	1	3	0	0.45
W 4	1457	2.0	37	16	48	1028	756	483	4	78	56	5	34	5	0.45
W 5	188	2.4	34	16	51	765	615	465	5	73	76	1	21	2	0.48
W 6	31	3.8	33	14	53	1006	778	551	8	122	85	9	5	1	0.45
W 7	14,184	1.8	37	24	39	1850	915	749	12	156	18	0	81	1	0.43
W 8	6262	2.3	32	17	52	1289	879	468	4	81	60	5	23	12	0.44
W 9	2,004	2.2	32	17	52	1218	862	485	6	62	54	12	33	1	0.46
W 10	1520	2.1	33	20	47	1131	868	604	6	60	43	0	53	4	0.43
W 11	927	1.9	32	17	52	1555	1058	564	9	120	72	2	25	1	0.40
W 12	3653	2.4	33	14	53	705	527	347	4	54	87	1	11	1	0.48
W 13	387	1.7	28	15	58	1555	1147	742	9	131	76	0	24	0	0.40
W 14	269	1.5	39	18	44	871	702	532	3	83	84	6	9	1	0.45
W 15	582	2.7	28	15	58	766	625	485	4	40	90	2	8	0	0.48
W 16	275	1.4	32	17	52	1288	1002	715	7	159	57	1	41	1	0.44
W 17	1586	1.8	39	18	44	1074	780	486	5	72	70	4	25	1	0.47
W 18	17,326	2.1	37	17	47	1721	1097	473	5	76	77	2	18	3	0.44
W 19	704	2.0	32	17	52	524	415	305	4	42	92	3	5	0	0.44
W 20	438	1.5	36	23	41	1335	753	182	11	157	15	0	85	0	0.47
W 21	443	1.8	33	14	53	1058	798	539	5	78	70	4	25	1	0.46
W 22	450	1.5	32	17	52	1273	1027	780	5	98	63	1	31	5	0.46
W 23	79	2.1	18	12	70	489	420	350	3	38	94	0	6	0	0.48
W 24	850	2.1	31	14	55	697	559	420	4	60	76	1	22	1	0.48
W 25	4295	2.1	32	17	52	1226	859	485	5	59	62	7	30	1	0.46
W 26	45	2.2	33	14	53	541	476	411	3	51	87	0	12	1	0.46

The percentages of urban area, forest cover (native and planted), and agricultural area (agriculture and pasture) were obtained from land use maps derived from the 4.1 collection of MapBiomas [30], with a resolution of 30 m, for the year 2018. In these 26 watersheds, variations of 3% to 85%, 5% to 96%, and 0% to 12% were found for forest cover, agriculture, and urban area, respectively. Mean NDVI (normalized difference vegetation Index) values were calculated for the native forest areas of the watersheds using Landsat 8 satellite images, with a resolution of 30 m, referring to the rainy period (January to March) and the dry period (July to August) of the year 2018 [31], with the mean of these two periods assigned to each watershed.

2.3. Climatic and Hydrological Data

The monthly precipitation data (mm) were estimated using CHIRPS (Climate Hazards Group InfraRed Precipitation with Station data—version 2.0 final) with 0.05° res-

olution satellite imagery [32], with average monthly flow (m^3/s) obtained in discharge stations of the 26 watersheds taken from the DAEE (Departamento de Águas e Energia Elétrica—Department of Water and Electricity) database for the period from 1980 to 2016. The annual flow was calculated from the average monthly flow normalized by the watershed area (mm/year). The potential evapotranspiration (mm) was calculated using the Thornthwaite (1948) method using the maximum air temperature and minimum air temperature (°C) data [33] with a spatial resolution of 0.25° × 0.25°, available for the period from 1980 to 2013, and from the NASA-POWER (National Aeronautics and Space Administration—Prediction Of Worldwide Energy Resource) database with a spatial resolution of 0.5° × 0.5°, used to fill the period from 2014 to 2016, as the first source was limited to the period from 1980 to 2013. All data were integrated in the annual scale. The entire data series of precipitation, potential evapotranspiration, and annual streamflow have the same data extension according to each watershed. The main limitation was the flow data, which ranged from 11 to 37 years. From the available annual streamflow data, the same years of rainfall and potential evapotranspiration data for watersheds were selected.

2.4. Hydrological Model

According to Budyko's framework [16,17], the actual evapotranspiration (E) is the result of a functional balance between the water supply in the atmosphere, represented by precipitation (P), and the energy availability of the system, represented by the potential evapotranspiration (PET). Thus, under conditions of adequate water supply, actual evapotranspiration will be limited by energy availability, while under conditions of adequate energy supply, actual evapotranspiration will be limited by water availability.

The need to better understand the dynamic of this function led to the emergence of several analytical solutions, such as the method of Fuh [6] adapted by Zhou [4]. The inversion of PET/P to P/PET offers some advantages. First, the PET value is always greater than zero and relatively stable in a given region, as it is determined by the available energy. On the other hand, P in some regions can reach zero, which could lead to infinite PET/P values, whereas using the P/PET makes it possible to define limiting values (minimum and maximum). Second, due to the difference in the boundary ranges, the use of P/PET allows for the most effective quantification of the hydrological sensitivity of R/P to P/PET instead of PET/P. In this work, the model of Fuh [6] rewritten by Zhou [4] was used on an annual basis (Equation (1)).

$$\frac{R}{P} = \left[1 + \left(\frac{\mathrm{P}}{PET}\right)^{-m}\right]^{\frac{1}{m}} - \left(\frac{\mathrm{P}}{\mathrm{PET}}\right)^{-1} \quad (1)$$

where P = precipitation (mm); PET = potential evapotranspiration (mm); R = streamflow (mm); and "m" is a dimensionless parameter that represents the physiographic features of the watershed.

2.5. Model Calibration and Validation

For model calibration, streamflow, potential evapotranspiration, and annual precipitation of the 26 watersheds were used in Equation (1) to determine the "m" values for the watersheds. The hydrological model was calibrated by selecting a random sample of 80% from the entire watershed database, leaving the remaining 20% for model validation. Validation was performed by comparing the R/P predicted by the model with the R/P recorded in the discharge stations (Figure S1), and three performance indicators were selected to validate the model: coefficient of determination (R^2); Willmott's index of agreement (d); and root mean square error (RMSE). After calibration and validation processes, a curve was fitted using simply R/P and P/PET to provide the "m" value for each watershed using nonlinear least squares with start at m = 2 [4]. The calculation was performed using the Rstudio interface (version 1.1.423) of R software.

2.6. Analysis of the "m" Value

A relationship was established between the "m" value and the water yield coefficient (R/P values) for all 26 watersheds. The physiographic features of the watersheds, with the same resolution data of 30 m (area, stream density, elevation, slope, land use, and NDVI), were related to the "m" values with a multiple linear regression model (stepwise method) and covariance analysis (Figures S2 and S3), and the relationship between the "m" value and hydrological resilience of the 26 watersheds was made using a threshold of elasticity (median of the elasticity values) and a threshold of "m" value taken from the median of 26 watersheds.

A sensitivity analysis of the hydrological response to P and PET was performed for two watersheds in the west of São Paulo (W10 and W20) and another two in the east of São Paulo (W12 and W19), which prescribed an increase/decrease of 20% in P and PET to predict the variability of "m" and the R/P coefficient.

2.7. Hydrological Resilience

Dynamic deviation and elasticity [3] were calculated to determine drought resistance and water yield resilience in the watersheds, respectively, but these metrics were adapted using the indexes of the hydrological model of Zhou [4]. In this study, two distinct temporal periods were defined for analysis: a cold period, consisting of five years with lower temperatures, and a warm period, encompassing five years marked by higher temperatures, for each watershed. This selection of five-year periods was made to emphasize responses potentially associated with interannual climate variability rather than responses to isolated and exceptional weather events, as supported by previous research [3,22]. Thus, the wetness index (WI) (precipitation/potential evapotranspiration = P/PET), which is reciprocal to the dryness index (DI) (potential evapotranspiration/precipitation = PET/P), and the water yield coefficient (*WYC*) (flow/precipitation = R/P), which corresponds to the evaporative index (EI) (actual evapotranspiration/precipitation = ET/P), was used to calculate the hydrological resilience [3,4,22].

Dynamic deviation is defined as the change in the water yield coefficient due to the change from the cold to the warm period, representing the watershed's resistance in terms of changes in water production to changes in climate (e.g., warming or drying).

Two components were calculated:

a. Static deviation (s) resulting from inherent characteristics of the watershed that are assumed to be constant over time, based on *WYC* observations from the cold period. Watersheds with $s < 0$ exhibit lower than expected water yield before warming based on predictions of the theoretical Budyko's curve ("m" values from 26 watersheds), while watersheds with $s > 0$ show water yield higher than expected.

$$s = WYC_{M,cool} - WYC_{B,cool} \quad (2)$$

where s corresponds to the static deviation; $WYC_{M,cool}$ corresponds to the average of the five cold years; and $WYC_{B,cool}$ corresponds to the value calculated from Budyko's curve of the cold period.

b. Dynamic deviation (d) obtained from changes in the watershed over time, considering the *WYC* of the warm period corrected by the static deviation (s). Dynamic deviation close to zero means high resistance to drought.

$$d = WYC_{M,warm} - WYC_{B,warm} - s \quad (3)$$

where d is the dynamic deviation; $WYC_{M,warm}$ is the average of the warm period; $WYC_{B,warm}$ is the value calculated from Budyko's curve of the warm period; and s corresponds to the static deviation.

Elasticity can be used as an indicator of hydrological resilience in watersheds in terms of predicting water yield under interannual climate variability conditions. Elasticity (e) was

calculated from the ratio between the variation in the wetness index (*WI*) and the water yield coefficient (*WYC*), encompassing the same periods of five cold and warm years. The elasticity of the watershed is the deviation from Budyko's curve following interannual climate variability (along the two axes of Budyko's theory).

$$e = (WI_{max} - WI_{min}) \,/\, (WYC_{R,max} - WYC_{R,min}) \quad (4)$$

where WI_{max} corresponds to the maximum value of the wetness index; WI_{min} corresponds to the minimum value of the wetness index; $WYC_{R,max}$ is the difference between the maximum value of the water yield coefficient and the maximum value of the water yield coefficient calculated from Budyko's curve ($WYC_{R,max} = WYC_{max} - WYC_{B,max}$); and $WYC_{R,min}$ is the difference between the minimum value of the water yield coefficient and the minimum value of the water yield coefficient calculated from Budyko's curve ($WYC_{R,min} = WYC_{min} - WYC_{B,min}$). A watershed exhibits high elasticity when its *WI* undergoes significant changes with climate warming, while the *WYC* changes only minimally. Conversely, a watershed demonstrates low elasticity when the *WYC* responds substantially to variations in *WI*. In this study, we employed the median elasticity value across all watersheds to evaluate the relative resilience of these hydrological systems.

3. Results

3.1. Model Calibration and Validation

From the calibration and validation of the hydrological model, it was possible to calculate the "m" values from the curves fitted for all watersheds using annual data. Figure 2 shows the scattering of annual R/P and P/PET for all watersheds. The average wetness index (P/PET) for all watersheds ranged from 0.8 to 1.5, the average water yield coefficient (R/P) ranged from 0.2 to 0.5, and the average "m" value ranged from 1.79 to 3.63, with median m = 2.96. The watershed with m = 3.63 (green curve in Figure 2) showed averages of P/PET = 1.2 and R/P = 0.3; thus, a large part of the rain evaporates and produces less flow as 30% of the rain. Meanwhile, the watershed with m = 1.79 (blue curve in Figure 2) showed averages of P/PET = 1.3 and R/P = 0.5; thus, comparatively, less of the rain is evaporated and more is converted to flow as 50% of the rain.

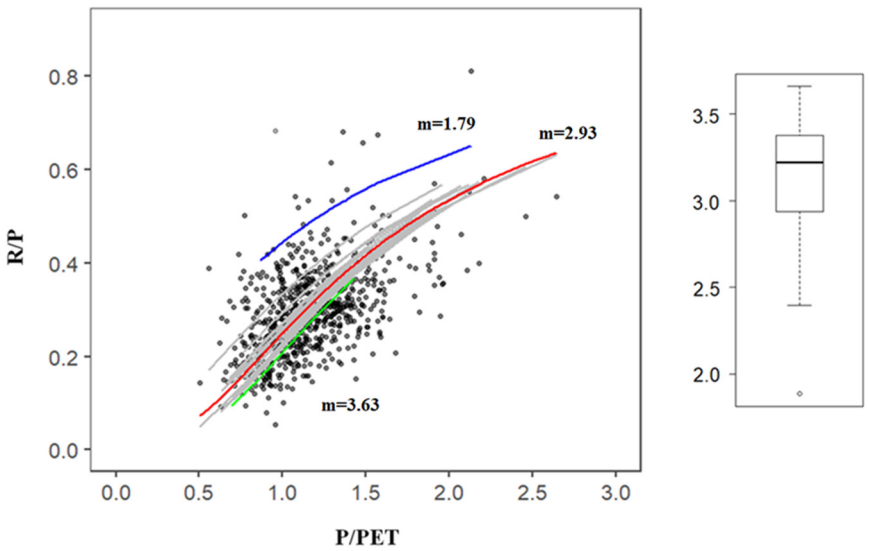

Figure 2. Curves (in gray) of the hydrological model fitted for all watersheds using annual data (black dots), with "m" values calculated for color curves. The red curve is the global curve with m = 2.93 ± 0.02 ($p < 0.001$) (average "m" value over the 26 watersheds); the blue and green curves represent watersheds with m = 1.79 and m = 3.63, respectively.

The R/P ratio represents the amount of rain that becomes streamflow in the long term. Figure 3 demonstrates a significant relationship between "m" values and the R/P ratio, with a coefficient of determination ($R^2 = 0.561$). Specifically, as the "m" value decreases, the R/P ratio increases, indicating an enhanced conversion of precipitation into streamflow. Additionally, it is noteworthy that data points exhibiting higher "m" values and lower R/P ratios are associated with elevated potential evapotranspiration (PET) values.

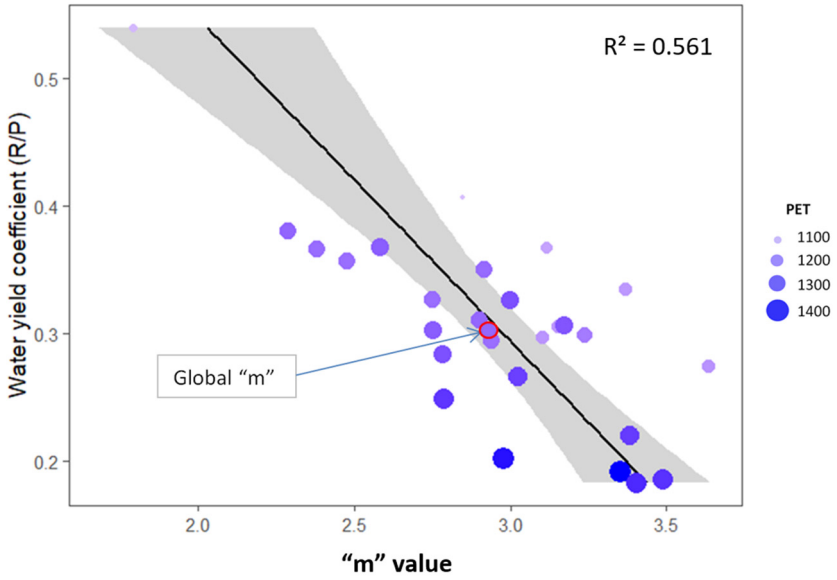

Figure 3. Relationship between the ratio of the water yield coefficient (R/P) to "m" value. Global "m" with m = 2.93 ± 0.02. The size of the circles represents the values of PET. The black line represents the trend of the relationship between the "m" value and the water yield coefficient. The gray area represents the confidence interval.

3.2. The Factors Influencing "m" and Sensitivity Analysis

From the fitted multiple regression model, we found a relationship between the mean elevation (m) and stream density (km km^{-2}), with the "m" values obtained for the 26 watersheds. These two physiographic features that correlated with the "m" value were statistically significant, with stream density controlling the prediction more (Table 2).

Table 2. Coefficients estimate, standard error, significance level, and coefficient of determination of the physiographic features of the watersheds.

Physiographic Features	Coefficients Estimate	Standard Error	Significance Level	Determination Coefficient
Mean elevation (A)	0.0009774	0.1190814	$p < 0.01$	$R^2 = 0.9791$
Stream density (B)	1.0959935	0.0003056	$p < 0.001$	

The sensitivity analysis (Figure 4) showed that, for watersheds with a high "m" value, W10 and W19, a decrease or increase of 20% in precipitation results in a greater decrease (−30% and −37%, respectively) or increase (27% and 38%, respectively) in R/P, respectively, while W12 and W20, which have low "m" values, resulted in a smaller decrease (−27% and −11%, respectively) or increase (26% and 9%, respectively) in R/P, respectively.

For potential evapotranspiration in W10 and W19, a decrease of 20% in PET results in an increase in R/P (34% and 47%, respectively), and an increase of 20% in PET results in a decrease in R/P (−25% and −31%, respectively); in W12 and W20, which have low "m" values, a decrease of 20% in PET results in an increase in R/P (32% and 11%, respectively) and an increase of 20% in PET results in a decrease (−23% and −9%, respectively) in R/P.

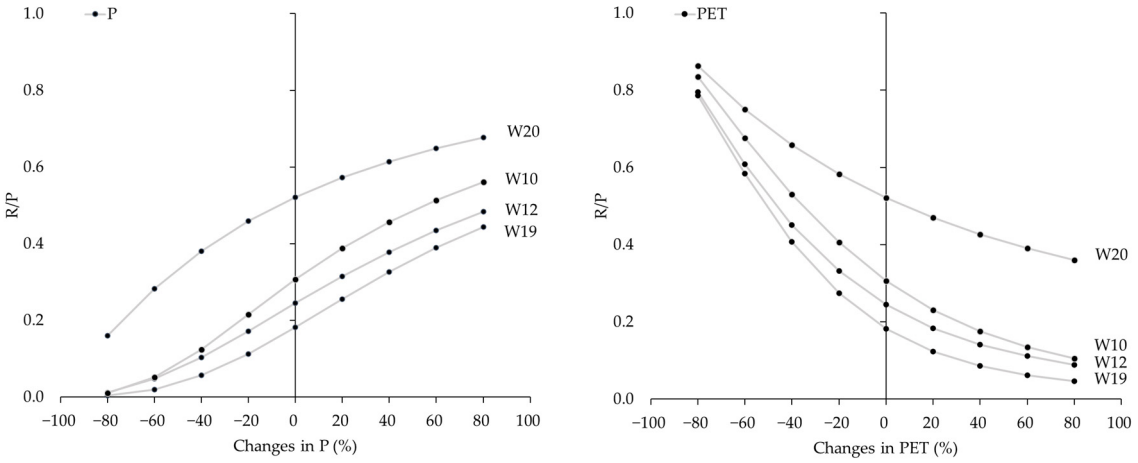

Figure 4. Sensitivity analysis for the watersheds W10 (m = 3.38), W12 (m = 2.79), W19 (m = 3.49), and W20 (m = 1.79), where the *X*-axis represents changes in percentage in P or PET. P denotes precipitation, R the streamflow, PET the potential evapotranspiration, and R/P the water yield coefficient.

3.3. Watershed's Hydrological Resilience

The values of static deviation (*s*) were obtained, for the 26 watersheds, which ranged between −0.04 and 0.15. Only two watersheds had $s < 0$ and, therefore, exhibit a lower-than-expected water yield before warming based on the predictions of Budyko's curve. The other 24 watersheds had a value of $s > 0$, which represents a higher-than-expected water yield from the predictions of Budyko's curve (Table 3).

Table 3. The dominant land use of each watershed is indicated (land use); five-year cool periods (characterized by the lowest average temperatures) and five-year warm periods (marked by the highest average temperatures); changes in temperature during shift from cool to warm period (ΔT), mean annual values of precipitation (P), potential evapotranspiration (PET), streamflow (R), water yield coefficient (R/P), and wetness index (P/PET); "m" values; and Budyko's metrics [static (*s*) and dynamic (*d*) deviations and elasticity (*e*)] of 26 watersheds.

Watershed	Land Use	Cool Period	Warm Period	ΔT (°C)	P (mm y^{-1})	PET (mm y^{-1})	R (mm y^{-1})	R/P	P/PET	m	s	d	e
W 1	Forest	1988–1992	2005–2009	0.4	1386	1268	407	0.29	1.09	2.94	0.06	−0.02	8.05
W 2	Agriculture	1990–1994	2006–2011	0.1	1424	1270	506	0.36	1.12	2.48	0.03	−0.04	2.98
W 3	Agriculture	1983–1992	1997–2006	1.0	1273	1435	233	0.18	0.89	3.40	0.08	−0.03	3.45
W 4	Forest	1992–1996	1998–2008	0.7	1432	1293	543	0.38	1.11	2.29	0.03	0.00	7.26
W 5	Agriculture	1991–1998	2007–2013	0.9	1394	1314	419	0.30	1.06	2.75	0.03	0.05	2.04
W 6	Agriculture	1989–1993	1995–2000	0.3	1432	1384	387	0.27	1.03	3.02	0.02	0.01	4.50
W 7	Forest	1989–1996	1999–2007	0.1	1533	1059	633	0.41	1.45	2.85	0.06	0.11	3.85
W 8	Agriculture	1988–1993	1995–2000	0.6	1563	1311	583	0.37	1.19	2.58	0.05	0.03	1.20
W 9	Agriculture	1986–1991	2005–2012	0.3	1384	1174	381	0.28	1.18	3.63	0.13	−0.07	3.56
W 10	Forest	1987–1993	2007–2014	0.1	1372	1165	425	0.31	1.18	3.15	0.08	0.02	3.44
W 11	Agriculture	1984–1995	2003–2012	0.2	1523	1160	519	0.34	1.31	3.37	0.15	−0.09	3.75
W 12	Agriculture	1991–1995	2004–2009	0.9	1284	1407	322	0.25	0.91	2.79	0.08	−0.09	1.93
W 13	Agriculture	1988–1999	2000–2007	0.8	1550	1134	576	0.37	1.37	3.12	0.14	−0.06	2.48
W 14	Agriculture	1981–1985	1986–1993	0.6	1589	1333	495	0.31	1.19	3.17	0.11	−0.06	3.02
W 15	Agriculture	1980–1987	2000–2009	1.3	1368	1394	305	0.22	0.98	3.38	0.14	−0.12	2.37
W 16	Forest	1989–1996	2011–2016	0.3	1612	1346	534	0.33	1.20	3.00	0.06	0.05	1.07
W 17	Agriculture	1989–1994	1998–2003	0.8	1426	1271	474	0.33	1.12	2.75	0.00	0.03	5.27
W 18	Agriculture	1981–1997	2004–2011	1.0	1461	1238	439	0.30	1.18	3.24	0.09	−0.05	4.88
W 19	Agriculture	1986–1993	2001–2007	0.9	1296	1418	243	0.19	0.91	3.49	0.03	0.06	0.94
W 20	Forest	1980–1988	1989–1994	0.1	1383	1077	767	0.55	1.28	1.79	−0.02	−0.02	4.25
W 21	Agriculture	1980–1986	1987–2013	0.3	1420	1272	526	0.37	1.12	2.38	0.04	−0.02	1.68
W 22	Agriculture	1985–1997	2003–2009	1.1	1593	1279	568	0.36	1.25	2.92	−0.04	0.16	5.57
W 23	Agriculture	1984–1991	2002–2006	1.4	1235	1476	250	0.20	0.84	2.98	0.05	−0.04	7.49
W 24	Agriculture	1989–1995	2007–2015	0.1	1364	1345	387	0.28	1.01	2.78	0.06	−0.09	2.51
W 25	Agriculture	1987–1991	2004–2008	0.2	1330	1169	404	0.30	1.14	3.10	0.08	−0.01	4.70
W 26	Agriculture	1994–2000	2002–2009	0.8	1338	1490	256	0.19	0.90	3.35	0.08	−0.03	3.15

The dynamic deviation values ranged between −0.12 and 0.16, representing the vertical deviation of the warm period in relation to Budyko's curve (after interannual climate variability). Of all the watersheds, 16 had $d < 0$; 1 watershed had $d = 0$; and 9 watersheds had $d > 0$.

The elasticity values ranged from 0.94 to 8.22, considering the median as being equal to 3.5; 13 watersheds showed values of $e < 3.5$, having low resilience, while the other 13 showed values of $e > 3.5$, having high resilience (Table 3).

4. Discussion

4.1. Model Calibration and Validation

The calibration and validation of the hydrological model obtained the following performance indicators: d equal to 0.75 (Willmott's index of agreement—the higher its value, the better the model's performance); R^2 equal to 0.33 (coefficient of determination); and RMSE of 0.08 (root mean square error). Several studies that used hydrological models obtained, after calibration and validation, d ranging from 0.68 to 0.96, R^2 ranging from 0.29 to 0.99, and [34–40] values comparable to those found in our study.

4.2. "m" Values of Watersheds

The results showed that two key physiographic features influence the "m" value and contribute to the water yield in the watersheds, and these characteristics can alter the water and energy balance of the watershed. The characteristics found were elevation and stream density. Elevation is an indicator of environmental conditions that can mainly affect the temperature gradient [40], showing a positive effect on water yield [41]. The slope can influence the soil water holding capacity and, consequently, the water residence time in the soil [4,42]. Lower slopes can contribute to water yield [43], while more pronounced slopes may cause significant changes in the flow [44]. The stream density is a key geomorphic characteristic that provides insights into soil texture and infiltration capacity, which indicates the extent of rivers (km) in the area of the watershed (km^2), and it generally has low values in regions with low permeability and flat relief [45]. Yildiz [46] found an increase in water yield with an increase in stream density. In comparison to other studies, Abatzoglou [47] found that precipitation seasonality, soil water holding capacity, topographic slope, and the fraction of snowfall were correlated with Budyko's framework parameter ("m" or "w" value). In another study assessing global patterns of climate and land cover effects on water yield, the results revealed a significant correlation between "m" values and forest cover, watershed slope, and watershed area [4]. And several studies have demonstrated strong correlations between "m" or "w" values and forest cover through the analysis of hydrometeorological variations and vegetation dynamics [39,48–52].

4.3. Watershed's Hydrological Resilience

In this study, elasticity values ranged from 0.94 to 8.22. Similar values were found, in the Eastern Mediterranean, with elasticity values ranging between 2.87 and 9.85, and the findings suggest that forests growing under consistently dry conditions may develop a range of hydrological and eco-physiological adaptations to drought, resulting in greater hydrological resilience [22]. In another study conducted in the upper Hailar River Basin, China, an elasticity value of 8.03 was reported; the analysis identified multiple factors influencing elasticity, with the key hydrological drivers being those that contribute to certain changes in evapotranspiration, including seasonal precipitation and eco-physiological dynamics [53]. All of these studies considered elastic watersheds with $e > 1$, and non-elastic watersheds are those that have a value of $e < 1$. In this study, an elasticity threshold equal to 3.5 was considered to represent more or less resilient watersheds, and not just represent watersheds with or without hydrological resilience.

The results demonstrate watershed responses to a transition in a short period of time from cold to warm conditions, providing a conceptual basis for understanding and predicting how interannual climate variability can affect water yield according to the

hydrological resilience of each watershed. Climate change can affect water yield in a watershed [54], but not all ecosystems will respond uniformly, because climate change varies geographically [55,56], and the type of vegetation, especially forests, can influence the streamflow [57,58].

The 26 watersheds have, on average, 65% of predominantly agricultural land use and 28% of forest area (including native and planted forests). In this study, the highest values of elasticity were found in watersheds with a higher percentage of forest cover. The same relationship was found in the study conducted by Creed [3], in which areas with different types of forests showed greater hydrological resilience, and older forests helped to minimize the effects of climate variations on evaporative rates. The main factors that influence elasticity are hydrological and ecological mechanisms, which are part of the physiographic features of watersheds and which involve the structure and composition of vegetation and anthropic action [3]. The anthropic factor that affects elasticity is land use in watersheds, such as agriculture and forests, and since water yield in the watershed tends to decrease with warming, vegetation will respond through transpiration, according to the evaporative demand of the system, being able to consume more or less water [59–61].

4.4. Study's Limitation

We recognize that this study's limitations may impact the inferences that can be drawn from this study, but they may also provide opportunities for new research. According to the multiple regression model of the physiographic features with the "m" values, there was no statistically significant correlation with land use (forest cover, agriculture, urban area, and NDVI), making it impossible to change (simulation) the "m" values from the change in the predominant land uses in each watershed. The main limitation was the low variation in forest cover in the 26 watersheds. Only 2 watersheds had more than 80% of forest cover; the other 24 watersheds varied from 3 to 53%, with a gradient of 50% to 100% of native forest cover missing. Several studies were able to find strong correlations between the parameters of Budyko's model with forest cover and NDVI, analyzing climatic variations and vegetation dynamics, using watersheds ranging from 30% to 100% forest cover, in order to quantify their effects on water yield in watersheds [39,48,49,51,52,62].

The sensitivity analysis showed that a smaller "m" value corresponds to a decrease in the hydrological response sensitivity to alterations in precipitation (P) and potential evapotranspiration (PET). This observation stands in contrast to the findings of Zhou [4], whose study indicated that within highly humid environments (P/PET > 1), hydrological responses exhibited minimal sensitivity to variations in the "m" value or the P/PET ratio. Conversely, in environments characterized by extreme drought conditions (P/PET < 1), their research revealed that lower "m" values were associated with an increased sensitivity of the R/P ratio to changes in both "m" and P/PET. We recognize that all the watersheds in this study are situated in humid environments (P/PET > 1); this limitation restricts the generalizability of our results and underscores further investigations in watersheds with more pronounced drought conditions.

4.5. Management Implications

According to the estimates of the population in Brazil, the population of the State of São Paulo is around 46 million, approximately 22% of the total population of Brazil. These people depend on water yield in watersheds, and the water supply will probably be affected by climate change [54]. In addition to the effects of climate change, forest and agricultural management activities can have significant consequences to the hydrological resilience of watersheds [63]. Some studies indicate that the increase in forest cover may reduce water yield in the watershed [64,65], but others suggest that there will be an increase in water yield from the production of moisture carried out by evapotranspiration, consequently contributing to cloud formation and precipitation [22,66]. In this study, it was possible to verify that the higher the "m" value, the lower the R/P ratio, which means that watersheds with higher "m" values have a low water yield, possibly due to physiographic features.

The relationship between the "m" value and hydrological resilience of the 26 watersheds can be observed in Figure 5, using a threshold of e = 3.5 (median of the elasticity values) and a threshold of m = 2.96 taken from the median of 26 watersheds. It is possible to observe that the watersheds in red have low resilience and a high "m" value (m > 2.96); in contrast, green watersheds are in a favorable situation, with high resilience and a low "m" value (m < 2.96), which means that the physiographic characteristics of these watersheds contribute to the water yield. Meanwhile, yellow watersheds represent intermediate situations, in which they have low resilience, but they also have a low "m" value (m < 2.96), or they have greater resilience but a high "m" value (m > 2.96).

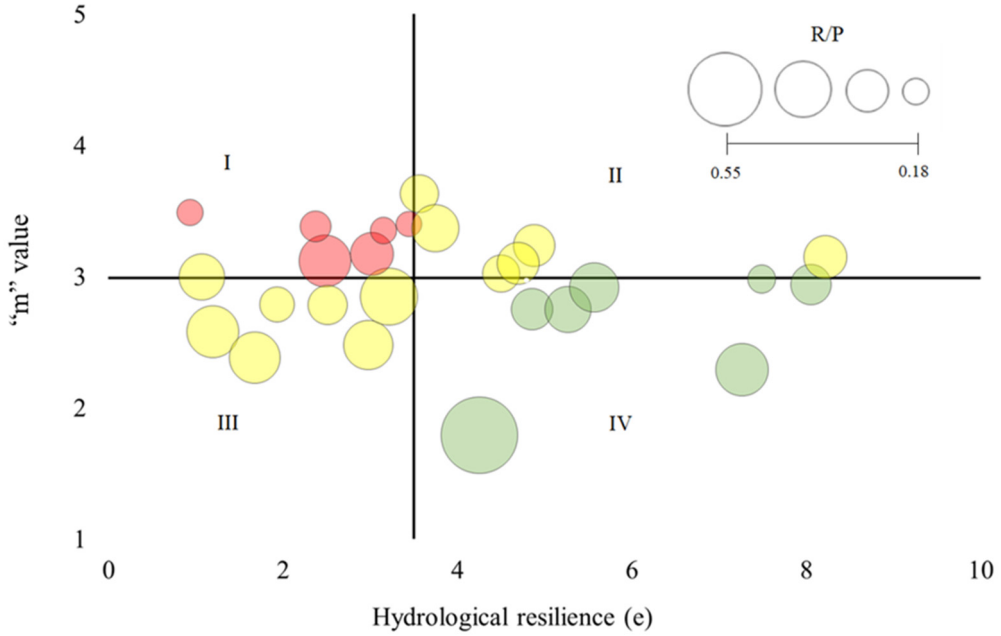

Figure 5. Relationship of "m" values with hydrological resilience (elasticity) of the 26 watersheds. The size of the circles represents the values of R/P (water yield coefficient). The red circles (I) represent watersheds with e < 3.5 and m > 2.96; yellow circles (II and III) represent watersheds with e > 3.5 and m > 2.96 and e < 3.5 and m < 2.96; and green circles (IV) represent watersheds with e > 3.5 and m < 2.96.

Budyko's metrics and the hydrological model provide a direction to assist the conservation and management of water resources under conditions of interannual climate variability, demonstrating important implications for understanding and predicting changes in water resources. Figure 5 and Table 4 can be used to identify sensitive areas for water yield, identified by quadrant I. These areas need greater attention in the management of water resources since land use activities, such as deforestation, agriculture, pasture, and urbanization, can have significant consequences for water yield [3,4]. Researchers have shown that in large watersheds, the change in forest cover has limited effects, no effect, or even positive effects on water yield [67–70]; thus, it is important to consider the type of vegetation present in the watershed, especially forests, as factors that influence the hydrological resilience and physiographic features of the soil [3,4]. Therefore, the addition of forest cover through forest restoration can help hydrological processes, increasing moisture, carried up by evapotranspiration and consequently contribute to precipitation [66], especially in humid tropical areas like the southeastern region of Brazil. Most of the watersheds in this study had P/PET values ranging from 0.8 to 1.4, and in these cases, the increase in forest cover can reduce the temperature of the Earth's surface and, consequently, decrease potential evapotranspiration [67,70,71].

Table 4. Description of the quadrants in Figure 5: watershed resilience, water availability, main purpose, and limitations of increased forest cover.

Quadrant	Watershed Resilience	Water Availability	Main Purpose of Increased Forest Cover	Limitations of Increased Forest Cover
I	Low	Low	-Improve resilience and physiographic features	-Restricted (However, could be increase diluted over time)
II	High	Low	-Improve physiographic features	-Allows increase of <30% in the watershed area
III	Low	High	-Improve resilience	-Allows increase of >30% in the watershed area
IV	High	High	-Improve flow regulation and water quality	-Not restricted

5. Conclusions

The hydrological model on the local scale responded even with small variations in the physiographic features of the watersheds, indicating the sensitiveness to these variations, allowing for recommendations for management practices to be made. Flow regionalization studies are normally used to grant rights to use water resources. However, these studies are based on past observed values and do not consider the effect of land use on water availability. Thus, models that consider the factors of global change are important complements for the sustainable water management of watersheds. The combination of "m" values and hydrological resilience contemplates the characteristic of water yield and becomes a strategy to adapt to global changes, identifying regions that are more sensitive to changes in climate and land use. Considering the change in land use with the removal or introduction of forests as a potential modifier of the evapotranspiration process, the results can assist in the definition of better strategies for the use of forests as mitigators of climate change for the maintenance of water yield in watersheds. The results of this study provide a basis to guide the planning of public policies aimed at water resources and to plan and guide land use in watersheds.

Supplementary Materials: The following supporting information can be downloaded at: https://www.mdpi.com/article/10.3390/su16208910/s1, Figure S1: Model validation through the relationship between predicted and observed values of R/P of the hydrological model. R^2 represents the coefficient of determination, "d" represents Willmott's index of agreement, and RMSE represents the root mean square error; Figure S2: Relationship between "m" value and physiographic features of the 26 watersheds; Figure S3: Diagnostic plots from linear regression analysis. The "Residuals vs. Fitted" plot shows the residuals spread around a horizontal line, indicating that the model is simulated in a way that meets the regression assumptions. The "Scale-Location" shows an almost horizontal line with spread points. The "Normal Q-Q" shows that residuals are normally distributed. The "Residuals vs. Leverage" shows that there is no influential case.

Author Contributions: Writing—original draft preparation, investigation, conceptualization, and project administration M.E.K.O.; writing—review and editing, E.M.M., H.R.R., X.W. and S.F.B.F.; visualization, formal analysis, data curation, and methodology, M.E.K.O. and E.M.M.; funding acquisition, M.E.K.O. and S.F.B.F. All authors have read and agreed to the published version of the manuscript.

Funding: This research was funded by the National Council for Scientific and Technological Development of Brazil, CNPq grant nº 133251/2018-7, and by São Paulo Research Support Foundation, FAPESP grant nº 2016/02877-5 and FAPESP grant nº 2018/10751-7.

Institutional Review Board Statement: Not applicable.

Informed Consent Statement: Not applicable.

Data Availability Statement: Data will be made available on request.

Acknowledgments: We would like to thank M.S.G. Otto and A. Vrechi for their valuable suggestions. This manuscript benefitted from the insightful suggestions of two anonymous reviewers.

Conflicts of Interest: Author Eduardo M. Mattos was employed by the company Geplant Forest Technology Ltd. The remaining authors declare that the research was conducted in the absence of any commercial or financial relationships that could be construed as a potential conflict of interest.

References

1. Sheldon, K.S. Climate Change in the Tropics: Ecological and Evolutionary Responses at Low Latitudes. *Annu. Rev. Ecol. Evol. Syst.* **2019**, *50*, 303–333. [CrossRef]
2. Marengo, J.A. Água e Mudanças Climáticas. *Estud. Avançados* **2008**, *22*, 83–96. [CrossRef]
3. Creed, I.F.; Spargo, A.T.; Jones, J.A.; Buttle, J.M.; Adams, M.B.; Beall, F.D.; Booth, E.G.; Campbell, J.L.; Clow, D.; Elder, K.; et al. Changing Forest Water Yields in Response to Climate Warming: Results from Long-Term Experimental Watershed Sites across North America. *Glob. Change Biol.* **2014**, *20*, 3191–3208. [CrossRef] [PubMed]
4. Zhou, G.; Wei, X.; Chen, X.; Zhou, P.; Liu, X.; Xiao, Y.; Sun, G.; Scott, D.F.; Zhou, S.; Han, L.; et al. Global Pattern for the Effect of Climate and Land Cover on Water Yield. *Nat. Commun.* **2015**, *6*, 1–9. [CrossRef] [PubMed]
5. Nobre, C.A.; Seller, P.J.; Shukla, J. Amazonian Deforestation and Regional Climate Change. *J. Clim.* **1991**, *4*, 957–988. [CrossRef]
6. Fuh, B. On the Calculation of the Evaporation from Land Surface. *Chin. J. Atmos. Sci.* **1981**, *5*, 23–31. [CrossRef]
7. Choudhury, B.J. Evaluation of an Empirical Equation for Annual Evaporation Using Field Observations and Results from a Biophysical Model. *J. Hydrol.* **1999**, *216*, 99–110. [CrossRef]
8. Costa, M.H.; Botta, A.; Cardille, J.A. Effects of Large-Scale Changes in Land Cover on the Discharge of the Tocantins River, Southeastern Amazonia. *J. Hydrol.* **2003**, *283*, 206–217. [CrossRef]
9. Wei, X.; Liu, W.; Zhou, P. Quantifying the Relative Contributions of Forest Change and Climatic Variability to Hydrology in Large Watersheds: A Critical Review of Research Methods. *Water* **2013**, *5*, 728–746. [CrossRef]
10. Zhang, M.; Liu, N.; Harper, R.; Li, Q.; Liu, K.; Wei, X.; Ning, D.; Hou, Y.; Liu, S. A Global Review on Hydrological Responses to Forest Change across Multiple Spatial Scales: Importance of Scale, Climate, Forest Type and Hydrological Regime. *J. Hydrol.* **2017**, *546*, 44–59. [CrossRef]
11. Zhang, L.; Dawes, W.R.; Walker, G.R. Response of Mean Annual Evapotranspiration to Vegetation Changes at Catchment Scale. *Water Resour. Res.* **2001**, *37*, 701–708. [CrossRef]
12. Zhang, M.; Wei, X. The Cumulative Effects of Forest Disturbance on Streamflow in a Large Watershed in the Central Interior of British Columbia, Canada. *Hydrol. Earth Syst. Sci. Discuss.* **2012**, *9*, 2855–2895. [CrossRef]
13. Hrachowitz, M.; Savenije, H.H.G.; Blöschl, G.; McDonnell, J.J.; Sivapalan, M.; Pomeroy, J.W.; Arheimer, B.; Blume, T.; Clark, M.P.; Ehret, U.; et al. A Decade of Predictions in Ungauged Basins (PUB)—A Review. *Hydrol. Sci. J.* **2013**, *58*, 1198–1255. [CrossRef]
14. Milly, P.C.D.; Dunne, K.A.; Vecchia, A.V. Global Pattern of Trends in Streamflow and Water Availability in a Changing Climate. *Nature* **2005**, *438*, 347–350. [CrossRef]
15. Domingues, L.M.; de Abreu, R.C.; da Rocha, H.R. Hydrologic Impact of Climate Change in the Jaguari River in the Cantareira Reservoir System. *Water* **2022**, *14*, 1286. [CrossRef]
16. Budyko, M.I. *The Heat Balance of the Earth's Surface*; U.S. Department of Commerce. National Weather Service: Washington, DC, USA, 1958.
17. Budyko, M.I. *Climate and Life*; Academic: San Diego, CA, USA, 1974.
18. Greve, P.; Gudmundsson, L.; Orlowsky, B.; Seneviratne, S.I. A Two-Parameter Budyko Function to Represent Conditions under Which Evapotranspiration Exceeds Precipitation. *Hydrol. Earth Syst. Sci.* **2016**, *20*, 2195–2205. [CrossRef]
19. Turc, L. Le Bilan d'eau Des Sols: Relations Entre Les Précipitations, l'évaporation et l'écoulement. *J. Hydraul.* **1955**, *3*, 36–44.
20. Pike, J.G. The Estimation of Annual Run-off from Meteorological Data in a Tropical Climate. *J. Hydrol.* **1964**, *2*, 116–123. [CrossRef]
21. Gerten, D.; Lucht, W.; Schaphoff, S.; Cramer, W.; Hickler, T.; Wagner, W. Hydrologic Resilience of the Terrestrial Biosphere. *Geophys. Res. Lett.* **2005**, *32*, 1–4. [CrossRef]
22. Helman, D.; Lensky, I.M.; Yakir, D.; Osem, Y. Forests Growing under Dry Conditions Have Higher Hydrological Resilience to Drought than Do More Humid Forests. *Glob. Change Biol.* **2017**, *23*, 2801–2817. [CrossRef]
23. Frauendorf, T.C.; MacKenzie, R.A.; Tingley, R.W.; Frazier, A.G.; Riney, M.H.; El-Sabaawi, R.W. Evaluating Ecosystem Effects of Climate Change on Tropical Island Streams Using High Spatial and Temporal Resolution Sampling Regimes. *Glob. Change Biol.* **2019**, *25*, 1344–1357. [CrossRef]
24. Tiezzi, R.O.; Barbosa, P.S.F.; Lopes, J.E.G.; Francato, A.L.; Zambon, R.C.; Silveira, A.; Menezes, P.H.B.J.; Isidoro, J.M.G.P. Trends of Streamflow under Climate Change for 26 Brazilian Basins. *Water Policy* **2019**, *21*, 206–220. [CrossRef]
25. Alvares, C.A.; Stape, J.L.; Sentelhas, P.C.; De Moraes Gonçalves, J.L.; Sparovek, G. Köppen's Climate Classification Map for Brazil. *Meteorol. Z.* **2013**, *22*, 711–728. [CrossRef]
26. Teixeira, A.A. Agência Nacional de Águas (ANA)-Catálogo de Metadados. Available online: https://metadados.snirh.gov.br/geonetwork/srv/por/catalog.search#/home (accessed on 15 August 2024).
27. USGS (U.S. Geological Survey). "SRTM Topography." SRTM Documentation, 2.1. Available online: https://earthexplorer.usgs.gov/ (accessed on 15 August 2024).

28. Hengl, T.; De Jesus, J.M.; Heuvelink, G.B.M.; Gonzalez, M.R.; Kilibarda, M.; Blagotić, A.; Shangguan, W.; Wright, M.N.; Geng, X.; Bauer-Marschallinger, B.; et al. SoilGrids250m: Global Gridded Soil Information Based on Machine Learning. *PLoS ONE* **2017**, *12*, e0169748. [CrossRef]
29. Rennó, C.D.; Nobre, A.D.; Cuartas, L.A.; Soares, J.V.; Hodnett, M.G.; Tomasella, J.; Waterloo, M.J. HAND, a New Terrain Descriptor Using SRTM-DEM: Mapping Terra-Firme Rainforest Environments in Amazonia. *Remote Sens. Environ.* **2008**, *112*, 3469–3481. [CrossRef]
30. Azevedo, C.B.; Enrique, M.T.; Miguel, A.L.U.; Jose, M.L.P. MapBiomas Brasil-Collection 4.1. Available online: https://brasil.mapbiomas.org/colecoes-mapbiomas-1 (accessed on 15 August 2024).
31. INPE (Instituto Nacional de Pesquisas Espaciais). INPE-Catálogo de Imagens. Available online: http://www.dgi.inpe.br/catalogo/explore (accessed on 15 August 2024).
32. Funk, C.; Peterson, P.; Landsfeld, M.; Pedreros, D.; Verdin, J.; Shukla, S.; Husak, G.; Rowland, J.; Harrison, L.; Hoell, A.; et al. The Climate Hazards Infrared Precipitation with Stations—A New Environmental Record for Monitoring Extremes. *Scientific Data* **2015**, *2*, 1–21. [CrossRef]
33. Xavier, A.C.; King, C.W.; Scanlon, B.R. Daily Gridded Meteorological Variables in Brazil (1980–2013). *Int. J. Climatol.* **2015**, *36*, 2644–2659. [CrossRef]
34. Deo, R.C.; Şahin, M. Application of the Artificial Neural Network Model for Prediction of Monthly Standardized Precipitation and Evapotranspiration Index Using Hydrometeorological Parameters and Climate Indices in Eastern Australia. *Atmos. Res.* **2015**, *161*, 65–81. [CrossRef]
35. Migue, F.E.; Maughan, M.; Bollero, G.A.; Long, S.P. Modeling Spatial and Dynamic Variation in Growth, Yield, and Yield Stability of the Bioenergy Crops Miscanthus × Giganteus and Panicum Virgatum across the Conterminous United States. *GCB Bioenergy* **2012**, *4*, 509–520. [CrossRef]
36. Singh, A.K.; Tripathy, R.; Chopra, U.K. Evaluation of CERES-Wheat and CropSyst Models for Water–Nitrogen Interactions in Wheat Crop. *Agric. Water Manag.* **2008**, *95*, 776–786. [CrossRef]
37. Yang, D.; Sun, F.; Liu, Z.; Cong, Z.; Ni, G.; Lei, Z. Analyzing Spatial and Temporal Variability of Annual Water-Energy Balance in Nonhumid Regions of China Using the Budyko Hypothesis. *Water Resour. Res.* **2007**, *43*, 4426. [CrossRef]
38. Potter, N.J.; Zhang, L.; Milly, P.C.D.; McMahon, T.A.; Jakeman, A.J. Effects of Rainfall Seasonality and Soil Moisture Capacity on Mean Annual Water Balance for Australian Catchments. *Water Resour. Res.* **2005**, *41*, 1–11. [CrossRef]
39. Li, D.; Pan, M.; Cong, Z.; Zhang, L.; Wood, E. Vegetation Control on Water and Energy Balance within the Budyko Framework. *Water Resour. Res.* **2013**, *49*, 969–976. [CrossRef]
40. Xu, X.; Liu, W.; Scanlon, B.R.; Zhang, L.; Pan, M. Local and Global Factors Controlling Water-Energy Balances within the Budyko Framework. *Geophys. Res. Lett.* **2013**, *40*, 6123–6129. [CrossRef]
41. Zengin, H.; Özcan, M.; Değermenci, A.; Bosque, T.Ç.-R. Undefined Effects of Some Watershed Characteristics on Water Yield in the West Black Sea Region of Northern Turkey. *Bosque* **2017**, *38*, 479–486. [CrossRef]
42. Shao, Q.; Traylen, A.; Zhang, L. Nonparametric Method for Estimating the Effects of Climatic and Catchment Characteristics on Mean Annual Evapotranspiration. *Water Resour. Res.* **2012**, *48*, 3517. [CrossRef]
43. Fan, M.; Shibata, H.; Chen, L. Spatial Priority Conservation Areas for Water Yield Ecosystem Service under Climate Changes in Teshio Watershed, Northernmost Japan. *J. Water Clim. Change* **2020**, *11*, 106–129. [CrossRef]
44. Caldwell, P.V.; Miniat, C.F.; Elliott, K.J.; Swank, W.T.; Brantley, S.T.; Laseter, S.H. Declining Water Yield from Forested Mountain Watersheds in Response to Climate Change and Forest Mesophication. *Glob. Change Biol.* **2016**, *22*, 2997–3012. [CrossRef]
45. Choto, M.; Fetene, A. Impacts of Land Use/Land Cover Change on Stream Flow and Sediment Yield of Gojeb Watershed, Omo-Gibe Basin, Ethiopia. *Remote Sens. Appl.* **2019**, *14*, 84–99. [CrossRef]
46. Yildiz, O. An Investigation of the Effect of Drainage Density on Hydrologic Response. *Turk. J. Eng. Environ. Sci.* **2004**, *28*, 85–94.
47. Abatzoglou, J.T.; Ficklin, D.L. Climatic and Physiographic Controls of Spatial Variability in Surface Water Balance over the Contiguous United States Using the Budyko Relationship. *Water Resour. Res.* **2017**, *53*, 7630–7643. [CrossRef]
48. Liang, W.; Bai, D.; Wang, F.; Fu, B.; Yan, J.; Wang, S.; Yang, Y.; Long, D.; Feng, M. Quantifying the Impacts of Climate Change and Ecological Restoration on Streamflow Changes Based on a Budyko Hydrological Model in China's Loess Plateau. *Water Resour. Res.* **2015**, *51*, 6500–6519. [CrossRef]
49. Zhang, S.; Yang, H.; Yang, D.; Jayawardena, A.W. Quantifying the Effect of Vegetation Change on the Regional Water Balance within the Budyko Framework. *Geophys. Res. Lett.* **2016**, *43*, 1140–1148. [CrossRef]
50. Silva, J.R.I.; Souza, R.M.S.; Santos, W.A.; de Almeida, A.Q.; de Souza, E.S.; Antonino, A.C.D. Aplicação Do Método de Budyko Para Modelagem Do Balanço Hídrico No Semiárido Brasileiro. *Sci. Plena* **2017**, *13*, 10. [CrossRef]
51. Wei, X.; Li, Q.; Zhang, M.; Giles-Hansen, K.; Liu, W.; Fan, H.; Wang, Y.; Zhou, G.; Piao, S.; Liu, S. Vegetation Cover—Another Dominant Factor in Determining Global Water Resources in Forested Regions. *Glob. Change Biol.* **2018**, *24*, 786–795. [CrossRef]
52. Xing, W.; Wang, W.; Zou, S.; Deng, C. Projection of Future Runoff Change Using Climate Elasticity Method Derived from Budyko Framework in Major Basins across China. *Glob. Planet. Change* **2018**, *162*, 120–135. [CrossRef]
53. Liu, J.; Xue, B.; Yinglan, A.; Sun, W.; Guo, Q. Water Balance Changes in Response to Climate Change in the Upper Hailar River Basin, China. *Hydrol. Res.* **2020**, *51*, 1023–1035. [CrossRef]

54. Aber, J.D.; Ollinger, S.V.; Federer, C.A.; Reich, P.B.; Goulden, M.L.; Kicklighter, D.W.; Melillo, J.M.; Lathrop, R.G. Predicting the Effects of Climate Change on Water Yield and Forest Production in the Northeastern United States. *Clim. Res.* **1995**, *05*, 207–222. [CrossRef]
55. Walther, G.R.; Post, E.; Convey, P.; Menzel, A.; Parmesan, C.; Beebee, T.J.C.; Fromentin, J.M.; Hoegh-Guldberg, O.; Bairlein, F. Ecological Responses to Recent Climate Change. *Nature* **2002**, *416*, 389–395. [CrossRef]
56. Loarie, S.R.; Duffy, P.B.; Hamilton, H.; Asner, G.P.; Field, C.B.; Ackerly, D.D. The Velocity of Climate Change. *Nature* **2009**, *462*, 1052–1055. [CrossRef]
57. Ewers, B.E.; Gower, S.T.; Bond-Lamberty, B.; Wang, C.K. Effects of Stand Age and Tree Species on Canopy Transpiration and Average Stomatal Conductance of Boreal Forests. *Plant Cell Environ.* **2005**, *28*, 660–678. [CrossRef]
58. Brown, A.E.; Zhang, L.; McMahon, T.A.; Western, A.W.; Vertessy, R.A. A Review of Paired Catchment Studies for Determining Changes in Water Yield Resulting from Alterations in Vegetation. *J. Hydrol.* **2005**, *310*, 28–61. [CrossRef]
59. Ford, C.R.; Hubbard, R.M.; Vose, J.M. Quantifying Structural and Physiological Controls on Variation in Canopy Transpiration among Planted Pine and Hardwood Species in the Southern Appalachians. *Ecohydrology* **2011**, *4*, 183–195. [CrossRef]
60. Swank, W.T.; Vose, J.M.; Elliott, K.J. Long-Term Hydrologic and Water Quality Responses Following Commercial Clearcutting of Mixed Hardwoods on a Southern Appalachian Catchment. *For. Ecol. Manag.* **2001**, *143*, 163–178. [CrossRef]
61. Polgar, C.A.; Primack, R.B. Leaf-out Phenology of Temperate Woody Plants: From Trees to Ecosystems. *New Phytol.* **2011**, *191*, 926–941. [CrossRef]
62. Liu, J.; Zhang, Q.; Singh, V.P.; Song, C.; Zhang, Y.; Sun, P.; Gu, X. Hydrological Effects of Climate Variability and Vegetation Dynamics on Annual Fluvial Water Balance in Global Large River Basins. *Hydrol. Earth Syst. Sci.* **2018**, *22*, 4047–4060. [CrossRef]
63. Fischer, J.; Lindenmayer, D.B.; Manning, A.D. Biodiversity, Ecosystem Function, and Resilience: Ten Guiding Principles for Commodity Production Landscapes. *Front. Ecol. Environ.* **2006**, *4*, 80–86. [CrossRef]
64. Filoso, S.; Bezerra, M.O.; Weiss, K.C.B.; Palmer, M.A. Impacts of Forest Restoration on Water Yield: A Systematic Review. *PLoS ONE* **2017**, *12*, e0183210. [CrossRef]
65. Li, Q.; Wei, X.; Zhang, M.; Liu, W.; Fan, H.; Zhou, G.; Giles-Hansen, K.; Liu, S.; Wang, Y. Forest Cover Change and Water Yield in Large Forested Watersheds: A Global Synthetic Assessment. *Ecohydrology* **2017**, *10*, e1838. [CrossRef]
66. Ellison, D.; Futter, M.N.; Bishop, K. On the Forest Cover–Water Yield Debate: From Demand- to Supply-Side Thinking. *Glob. Change Biol.* **2012**, *18*, 806–820. [CrossRef]
67. Wang, S.; Fu, B.J.; He, C.S.; Sun, G.; Gao, G.Y. A Comparative Analysis of Forest Cover and Catchment Water Yield Relationships in Northern China. *For. Ecol. Manag.* **2011**, *262*, 1189–1198. [CrossRef]
68. Ceballos-Barbancho, A.; Morán-Tejeda, E.; Luengo-Ugidos, M.Á.; Llorente-Pinto, J.M. Water Resources and Environmental Change in a Mediterranean Environment: The South-West Sector of the Duero River Basin (Spain). *J. Hydrol.* **2008**, *351*, 126–138. [CrossRef]
69. Buttle, J.M.; Metcalfe, R.A. Boreal Forest Disturbance and Streamflow Response, Northeastern Ontario. *Can. J. Fish Aquat. Sci.* **2011**, *57*, 5–18. [CrossRef]
70. Zhou, G.; Wei, X.; Luo, Y.; Zhang, M.; Li, Y.; Qiao, Y.; Liu, H.; Wang, C.; Zhou, C.; Wei, X.; et al. Forest Recovery and River Discharge at the Regional Scale of Guangdong Province, China. *Water Resour. Res.* **2010**, *46*, 9503. [CrossRef]
71. Peng, S.S.; Piao, S.; Zeng, Z.; Ciais, P.; Zhou, L.; Li, L.Z.X.; Myneni, R.B.; Yin, Y.; Zeng, H. Afforestation in China Cools Local Land Surface Temperature. *Proc. Natl. Acad. Sci. USA* **2014**, *111*, 2915–2919. [CrossRef]